EMAP: A 3-D, Finite Element Modeling Code for Analyzing Time-Varying Electromagnetic Fields

Todd Hubing, Mohammad Ali, and Girish Bhat
University of Missouri-Rolla
Rolla, Missouri 65401

Introduction

EMAP (ElectroMagnetic Analysis Program) is a three-dimensional finite element modeling code that was developed as a tool to be used for education and research. Like commercial finite element modeling codes, it solves for the field distribution in a variety of bounded, 3-dimensional geometries. Unlike commercial finite element modeling codes however, it is relatively easy to learn to use and it is distributed in source code form. EMAP can be used for student projects and demonstrations in undergraduate electromagnetics courses or in graduate microwave system courses. It is also a very useful laboratory aid for courses in numerical modeling techniques.

EMAP is not intended to compete with commercial codes. It does not have a sophisticated mesh generator, graphical output, or unlimited technical support. The purpose of the EMAP code is to provide an affordable tool that students can use to learn about electromagnetics and finite element modeling.

There are currently three versions of the EMAP code. EMAP-1 uses a variational formulation described by Maile [1]. EMAP-2 employs the Galerkin formulation described in papers by Paulsen and Lynch [2,3]. EMAP-2P is a parallel version of EMAP-2 designed to run on the Intel hypercube platforms. Each of these codes employ tetrahedral, first-order, nodal elements. The EMAP-1 code effectively demonstrates the problem of 'vector parasites' or 'spurious modes' that often arise in finite element modeling. EMAP-2 and EMAP-2P have been formulated to eliminate the vector parasite problem. EMAP-1 and EMAP-2 are written in 'C' and can be compiled and run on PCs, workstations, or mainframes.

The EMAP codes are readily available to educational and research institutions. They can be freely copied or distributed in unmodified form.

Structure of the EMAP code

The finite element mesh is defined on a cartesian grid using brick-shaped elements (hexahedra). The EMAP code automatically subdivides each hexahedron into five tetrahedra as shown in Figure 1. Linear functions of electric field strength with unknown coefficients at each node are the basic building blocks of the finite element solution. A matrix equation relating constants derived from the fixed (or constrained) node coefficients to linear functions of the unconstrained node coefficients is derived using one of the procedures outlined in the following sections.

The code is modular and both EMAP-1 and EMAP-2 follow the same basic solution procedure. A flowchart outlining the basic structure of the EMAP codes is provided in Figure 2. Specific

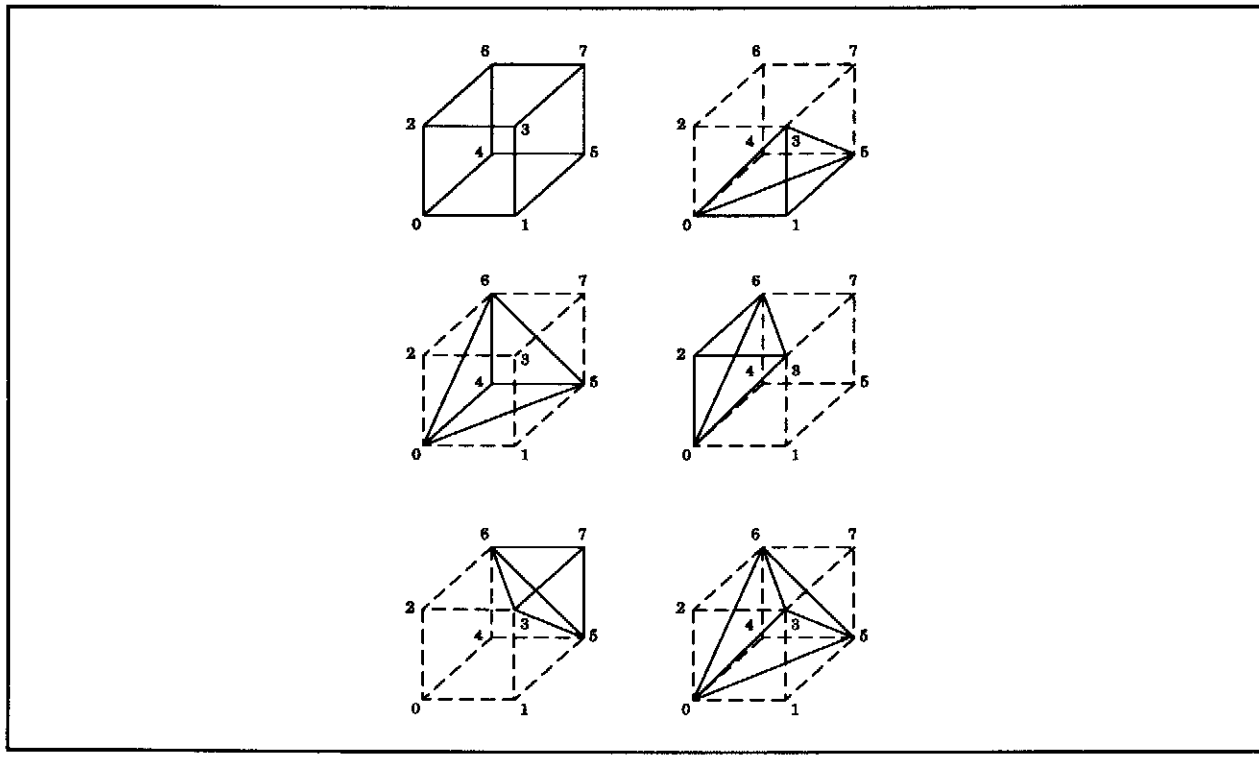

Figure 1: Division of hexahedron into 5 tetrahedra

subroutines are assigned to each task in the chart. Note that many subroutines are common to both EMAP-1 and EMAP-2. A brief description of each subroutine is provided below:

initialize	Reads the data input file and initializes variables.
no_of_hex	Calculates the number of hexahedra and number of global nodes.
assign.dim	Assigns to each node a global coordinate (x,y,z) and stores the result in the array asdnco[].
hex_nodes	Assigns each vertex of every hexahedra a unique global node number and stores the result in the array hexhed[].
div.hex	Divides a hexahedra into 5 tetrahedra and assigns node numbers based on connectivity. Node numbers are stored in the array tetrnod[].
vol.det	Calculates the volume determinant of the specified tetrahedron
cofac	Calculates the cofactors of the specified tetrahedron matrix
A.matrix	Calculates the tetrahedral matrix coefficients (12 x 12 matrix).
hex_max	Assembles the hexahedron matrix.
global.mat	Assembles the global matrix exploiting the sparsity to reduce the memory required.
cal.nodes	Determines which nodes are free, forced or boundary nodes and stores their node numbers in the arrays unodes[], fnodes[], and bfnodes[] respectively. Values of forced nodes are stored in the array forval[].

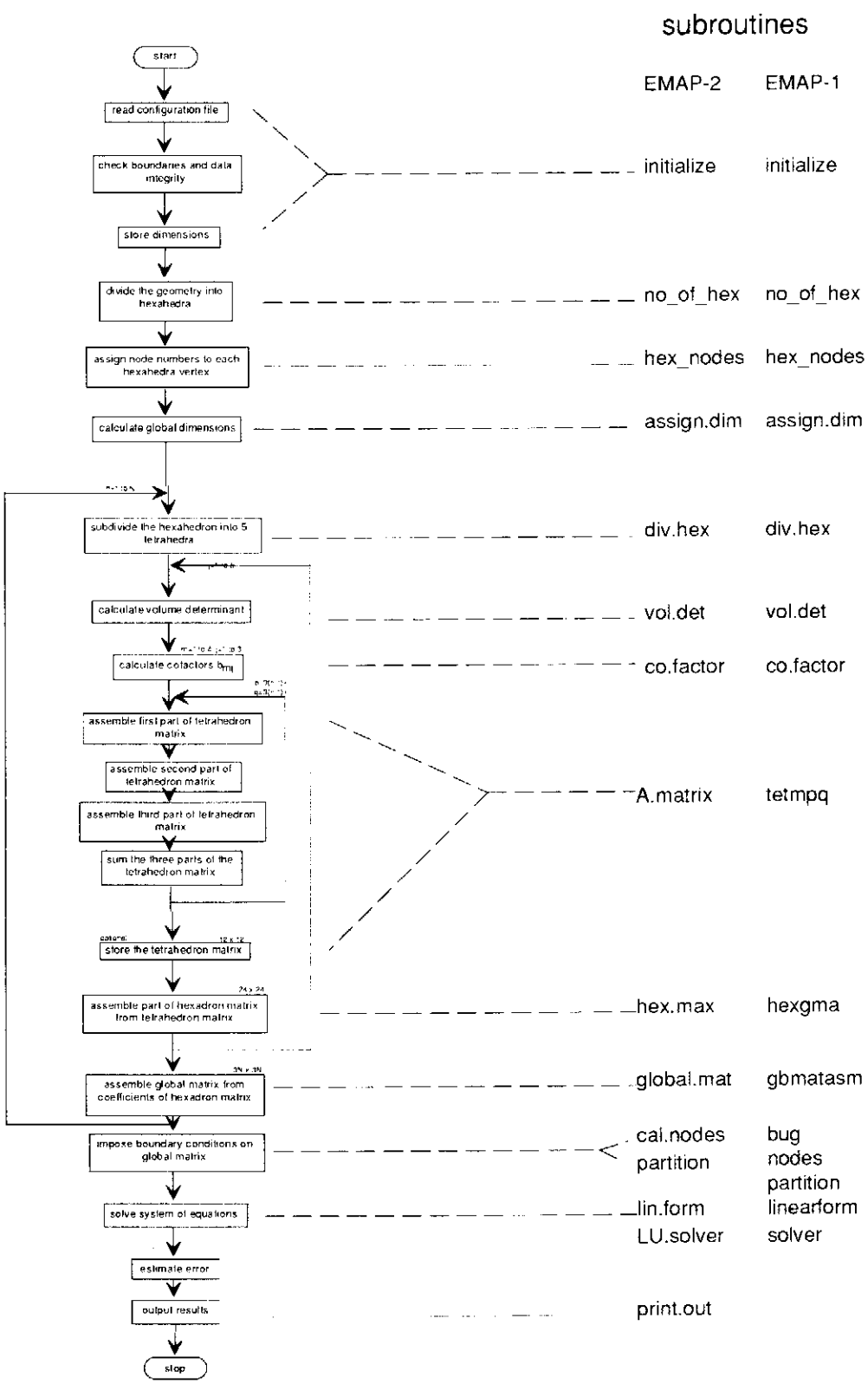

Figure 2: Flowchart for EMAP-1 and EMAP-2 codes

partition	Partitions the global matrix
lin.form	Prepares a matrix equation of the form Ax=B.
LU.solver	Solves the linear system of equations. Currently this is done using an LU-decomposition technique.
print.out	Formats and prints the electric field coefficients at each node.

EMAP-1 Formulation

EMAP-1 employs the variational formulation described by Maile [1]. Variational methods solve for the field distribution using a suitable *functional*. The functional is a function of the field distribution that is known to be stationary (i.e. has a minimum or maximum value) when the distribution is the *true* solution. Generally, the functional is an expression relating to the total energy in the configuration. The functional used by the EMAP-1 code is of the form,

$$F_E = \frac{1}{2}\int_v \varepsilon \left[E\cdot E^* - \frac{(\nabla\times E)\cdot(\nabla\times E^*)}{k^2} \right] dv \tag{1}$$

where E is the electric field distribution, ε is the permittivity of the material and k is the wave number ($k = \omega\sqrt{\varepsilon\mu}$). To determine the field distribution that minimizes this functional, this expression must be partially differentiated with respect to the vector components of E and the resulting expression set equal to zero. Using the procedures and notation of Maile [1], which is also described in the text by Silvester and Ferrari [4], the discretized partial derivative of the E-field functional in a tetrahedral element is given by,

$$\frac{\delta F_E}{\delta E_m^{(i)}} = \varepsilon V\left(\frac{1+\delta_{mn}}{20}\right)E_n^{(i)} - \frac{\varepsilon\,(b_{mj}b_{nj}E_n^{(i)} - b_{mk}b_{ni}E_n^{(k)})}{36Vk^2} \tag{2}$$

where $E_m^{(i)}$ is the i^{th} component of **E** at the m^{th} vertex. i,j,k each take on values of 1,2,3 and m,n range from 1 to 4. V is the volume of the tetrahedron. b_{mj}, b_{nj}, b_{mk}, and b_{ni} represent cofactors of the volume determinant. The expression in Equation 2 is used to find the coefficients of a tetrahedron submatrix of order 12 (4 tetrahedron vertices x 3 vector field components).

Partial derivative coefficients are evaluated for each tetrahedral element. The tetrahedron submatrices are then assembled into hexahedron submatrices, which are subsequently assembled to form a global matrix. A matrix equation is then formed which equates these coefficients to zero, thus enforcing the stationary condition.

The global matrix at this point is singular. The system of equations cannot be solved until a sufficient set of boundary conditions is applied. This involves constraining the electric field at some nodes to take on a particular value. Generally, the tangential component of electric field is constrained to have a value of zero on metallic boundaries. Sources are included in the model by constraining the field at some nodes to take on a fixed non-zero value.

After imposing boundary conditions, the matrix equation can be put in the form **Ax=B** where **x** is a vector of coefficients describing the electric field at each unforced node. The coefficients of **A** and **B** are known functions of the problem geometry, mesh geometry and boundary conditions. Solving the matrix equation for **x** yields the coefficients necessary to describe the field distribution throughout the problem region.

EMAP-2 Formulation

EMAP-2 does not employ a variational method. Instead it applies a Galerkin method to solve a modified form of the vector Helmholtz equation introduced by Paulsen and Lynch [3]. The modified form below includes a term which explicitly enforces the condition that $\nabla \cdot \boldsymbol{E}$ must be 0 in a homogeneous medium,

$$\nabla \times \left(\frac{1}{j\omega\mu} \nabla \times \boldsymbol{E} \right) - \nabla \left(\frac{1}{j\omega\mu\varepsilon} \nabla \cdot \varepsilon \boldsymbol{E} \right) + j\omega\varepsilon \boldsymbol{E} = 0 \tag{3}$$

The expanded weak form of this equation used by the EMAP-2 code can be written as,

$$< \frac{1}{j\omega\mu} (\nabla \times \boldsymbol{E}) \times \nabla \varphi_i > + < \frac{1}{j\omega\mu\varepsilon} (\nabla \cdot \varepsilon \boldsymbol{E}) \nabla \varphi_i > + < j\omega\varepsilon \boldsymbol{E} \, \varphi_i > = 0 \tag{4}$$

where < and > indicate integration over the problem domain. φ_i are the basis functions associated with the Galerkin procedure (in this case the linear field distribution associated with each finite element).

Expanding **E** in terms of weighting functions φ_j such that,

$$\boldsymbol{E} = \sum_{j=1}^{N} E_j \, \varphi_j \tag{5}$$

and substituting for the electric field in Equation 3, results in an expression that can be written in matrix form as $A_{ij} E_j = 0$ where,

$$A_{ij} = \begin{bmatrix} < \frac{\delta\varphi_j}{\delta x}\frac{\delta\varphi_i}{\delta x} + \frac{\delta\varphi_j}{\delta y}\frac{\delta\varphi_i}{\delta y} + \frac{\delta\varphi_j}{\delta z}\frac{\delta\varphi_i}{\delta z} - k^2\varphi_j\varphi_i > & < \frac{\delta\varphi_j}{\delta x}\frac{\delta\varphi_i}{\delta y} + \frac{\delta\varphi_j}{\delta y}\frac{\delta\varphi_i}{\delta x} > & < \frac{\delta\varphi_j}{\delta x}\frac{\delta\varphi_i}{\delta z} + \frac{\delta\varphi_j}{\delta z}\frac{\delta\varphi_i}{\delta x} > \\ < \frac{\delta\varphi_j}{\delta y}\frac{\delta\varphi_i}{\delta x} + \frac{\delta\varphi_j}{\delta x}\frac{\delta\varphi_i}{\delta y} > & < \frac{\delta\varphi_j}{\delta x}\frac{\delta\varphi_i}{\delta x} + \frac{\delta\varphi_j}{\delta y}\frac{\delta\varphi_i}{\delta y} + \frac{\delta\varphi_j}{\delta z}\frac{\delta\varphi_i}{\delta z} - k^2\varphi_j\varphi_i > & < \frac{\delta\varphi_j}{\delta y}\frac{\delta\varphi_i}{\delta x} + \frac{\delta\varphi_j}{\delta z}\frac{\delta\varphi_i}{\delta y} > \\ < \frac{\delta\varphi_j}{\delta z}\frac{\delta\varphi_i}{\delta x} + \frac{\delta\varphi_j}{\delta x}\frac{\delta\varphi_i}{\delta z} > & < \frac{\delta\varphi_j}{\delta z}\frac{\delta\varphi_i}{\delta y} + \frac{\delta\varphi_j}{\delta y}\frac{\delta\varphi_i}{\delta z} > & < \frac{\delta\varphi_j}{\delta x}\frac{\delta\varphi_i}{\delta x} + \frac{\delta\varphi_j}{\delta y}\frac{\delta\varphi_i}{\delta y} + \frac{\delta\varphi_j}{\delta z}\frac{\delta\varphi_i}{\delta z} - k^2\varphi_j\varphi_i > \end{bmatrix} \tag{6}$$

The entries in this matrix can be expressed as functions of the tetrahedral element volume (V) and the corresponding cofactors (b_l,c_l,d_l) [5] resulting in the expression below,

$$A_{ij} = \begin{bmatrix} \frac{b_i b_i^T + c_i c_i^T + d_i d_i^T}{36V} - \begin{cases} 1/10 & i=j \\ 1/20 & i \neq j \end{cases} & \frac{-b_i c_i^T + c_i b_i^T}{36V} & \frac{-b_i d_i^T + d_i b_i^T}{36V} \\ \frac{-c_i b_i^T + b_i c_i^T}{36V} & \frac{b_i b_i^T + c_i c_i^T + d_i d_i^T}{36V} - \begin{cases} 1/10 & i=j \\ 1/20 & i \neq j \end{cases} & \frac{-c_i d_i^T + d_i c_i^T}{36V} \\ \frac{-d_i b_i^T + b_i d_i^T}{36V} & \frac{-d_i c_i^T + c_i d_i^T}{36V} & \frac{b_i b_i^T + c_i c_i^T + d_i d_i^T}{36V} - \begin{cases} 1/10 & i=j \\ 1/20 & i \neq j \end{cases} \end{bmatrix} \quad (7)$$

Assembly of the hexahedron matrices and global matrix proceeds in the same manner as EMAP-1. In fact, although EMAP-1 and EMAP-2 are very different in terms of their solution method, only two subroutines are significantly different in the two codes. The subroutines that calculate the cofactors and create the tetrahedral submatrix are necessarily completely different. The subroutines that read the data, define the elements, and assemble and solve the matrix equation are virtually identical.

One additional difference between EMAP-1 and EMAP-2 is that the EMAP-2 code permits the electric field to be discontinuous at a dielectric boundary. This feature significantly improves the codes' ability to model configurations with dielectric interfaces. The procedure used is similar to that described by Paulsen [6]. Nodes on a dielectric interface are effectively split in two during the initial stages of the algorithm. Each half of the split node is in a different dielectric. During the final stages of the global matrix assembly, the halves are recombined and the discontinuity in the normal electric field is explicitly enforced.

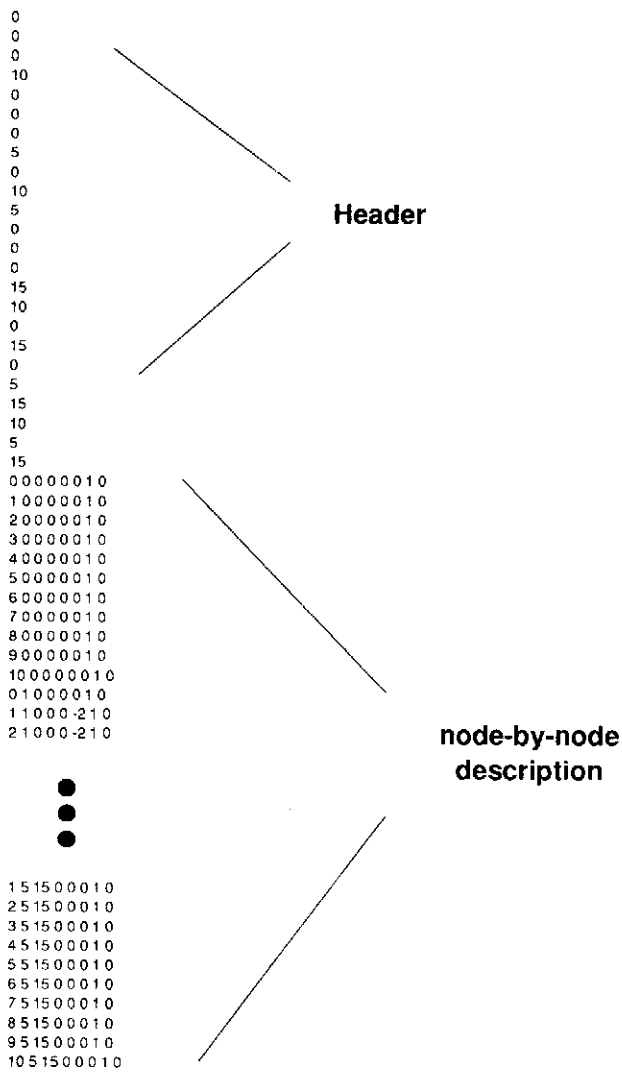

Figure 3: Sample data input listing

Data Input and Output

The EMAP codes read data in as an ASCII text file and print data out in the same form. This allows the source code to remain free of non-standard graphical I/O commands or routines. As a result, the EMAP source code is highly portable and has been run on a variety of platforms without modification.

The basic format of the input data is a short header followed by a list of the mesh node coordinates. A sample input file is illustrated in Figure 3.

Because it can be difficult and time consuming to create an error-free data input file for 3-D configurations, a translation code has been written that allows the user to draw the input configuration using a commercial com-

puter aided drawing program. DesignCAD 3-D [7] is a powerful, but relatively easy to learn CAD program that can be used to generate fairly complex 3-D geometries. The translation code reads the DesignCAD output file and creates an EMAP data input file. The translation code associates DesignCAD grid points with mesh nodes. Colors in the CAD drawing are used to represent different material properties and arrows are used to provide excitation sources [8].

The DesignCAD interface has proven to be an invaluable aid for creating and verifying input configurations. DesignCAD 3-D runs on PCs and Macintoshes and is available to educational institutions at a nominal charge. It is also possible to develop translation codes for other CAD programs running on other platforms. In many cases, the effort involved in writing a new translation code is less than the effort required to learn to use a non-standard graphical interface.

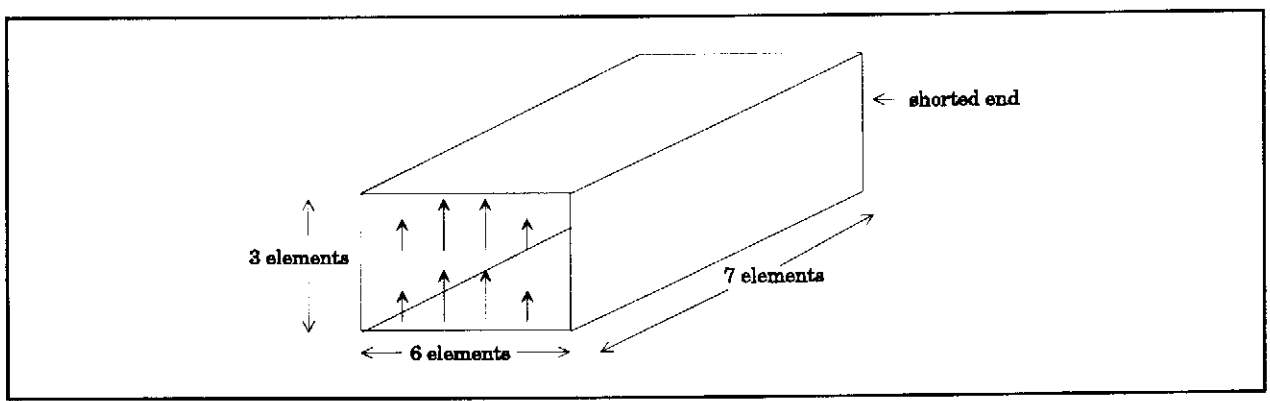

Figure 4: Shorted, air-filled waveguide of Example 1

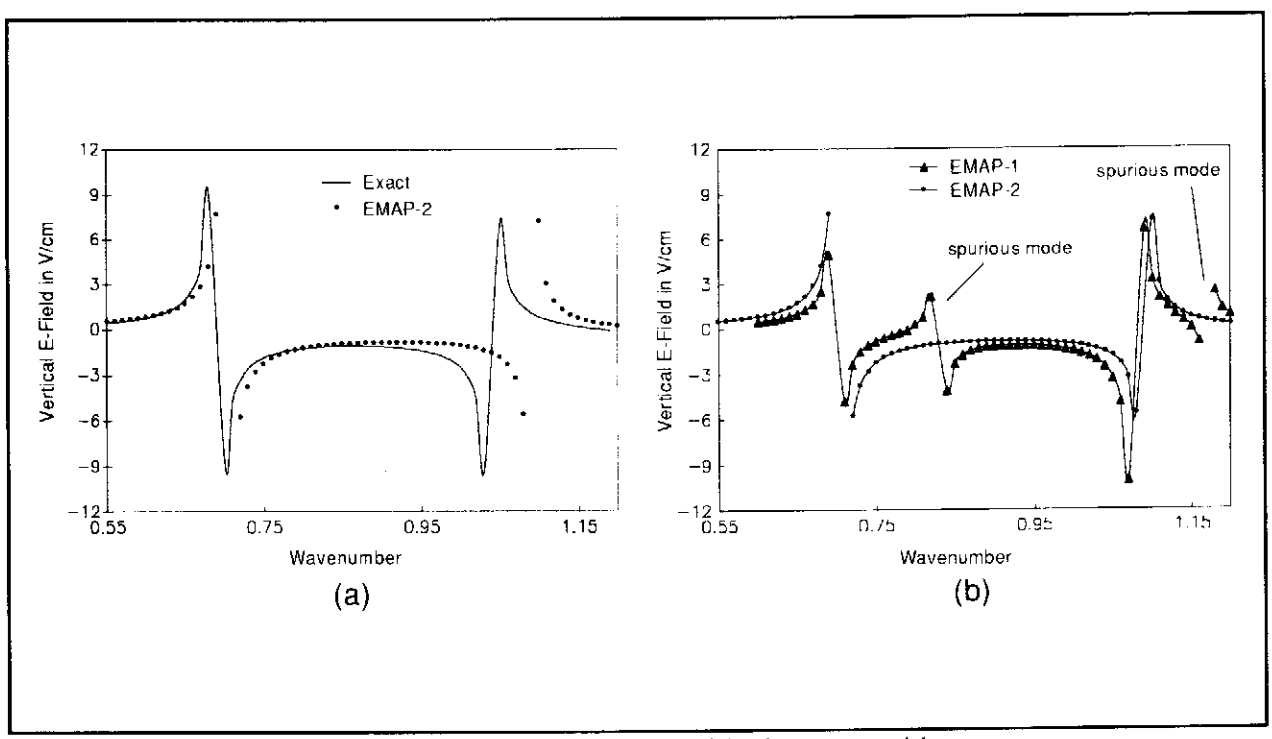

Figure 5: Field at a point inside the waveguide

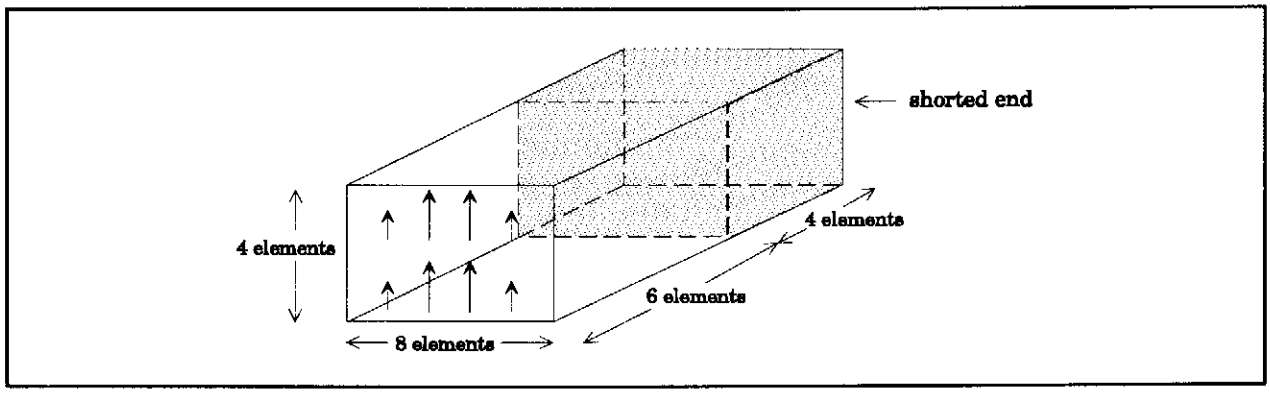

Figure 6: Waveguide with dielectric loading

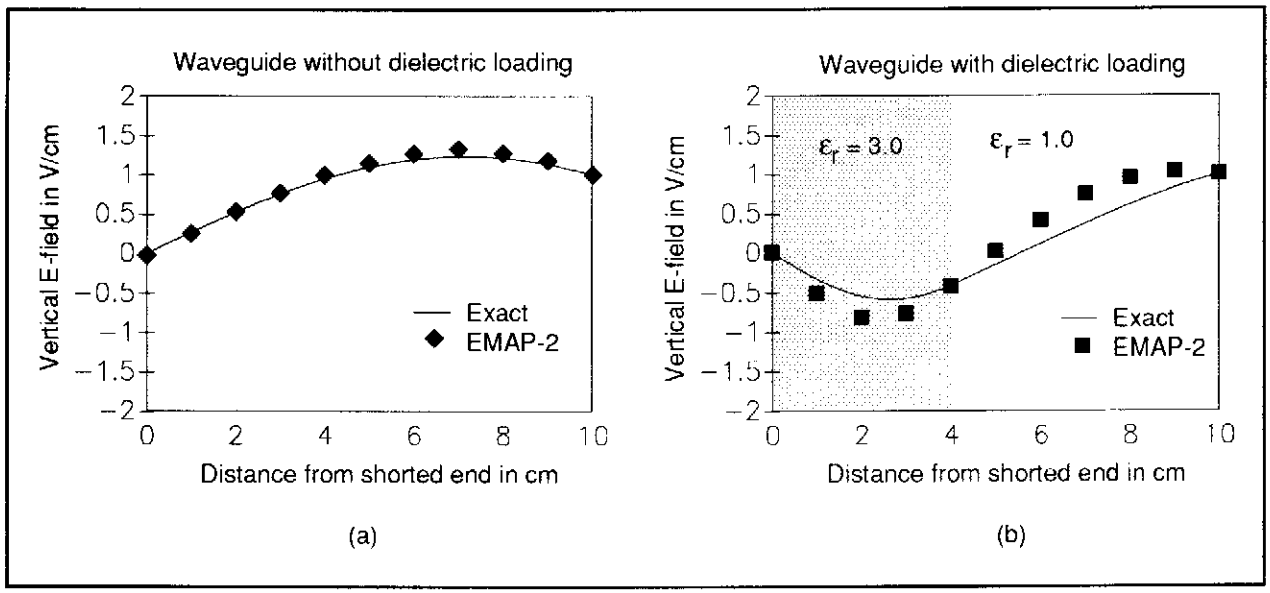

Figure 7: Vertical E-field in dielectric loaded waveguide

Output from the EMAP code consists of a listing of the node coordinates and the electric field strength at each node. This data can be easily read by a variety of spreadsheet programs and rearranged, plotted, or manipulated as desired.

Examples

As an illustration of how the EMAP codes can be used, two sample configurations are analyzed below. The first configuration is a TE_{10} wave propagating in an air-filled waveguide shorted at one end (see Figure 4). Despite the relatively crude finite element mesh and the small number of elements used to model this configuration, fairly good agreement is obtained between the EMAP-2 calculated field and an exact analytical calculation as shown in Figure 5a. This figure shows the vertical electric field at a point 3 cm away from the shorted end as a function of wave number, k. Note that the frequency of the first resonance shown is predicted very accurately even though at this frequency each element is 1/7th of a wavelength long. At the second resonance, where each element is greater than 1/5th of a wavelength, there is understandably significant error. A finer mesh is required to analyze this structure at these higher frequencies. Figure 5b compares the EMAP-2 results with the results from EMAP-1. Spurious modes in the EMAP-1 results are clearly observed.

This configuration is particularly prone to spurious modes at the higher wavenumbers where modes other than TE_{10} are supported.

The second sample configuration is the dielectric loaded waveguide illustrated in Figure 6. This waveguide is also shorted at one end and driven in the TE_{10} mode. The vertical electric field strength is plotted as a function of position along the center of the waveguide in Figure 7. With or without the dielectric loading, there is very good agreement between the finite element model and analytical results calculated using standard transmission line theory.

Conclusions

The EMAP codes have been developed to fill a need for an easy-to-learn and use, 3-D electromagnetic finite element modeling code. EMAP is primarily intended for use in education, but the technique is powerful enough for a variety of applications.

EMAP-1 is a variational formulation exhibiting spurious mode phenomena, while EMAP-2 is a Galerkin formulation that is immune to spurious modes. Both versions are distributed in source code form and run on a variety of platforms. These codes are available by anonymous ftp from *emclab.ee.umr.edu*. In the near future, they should be available on diskette through the Applied Computational Electromagnetics Society (ACES) and the Center for Computer Applications in Electromagnetics Education (CAEME).

References

[1] G. L. Maile, "Three-Dimensional Analysis of Electromagnetic Problems by Finite element Methods," Ph.D. Dissertation, University of Cambridge, U.K., Dec. 1979.

[2] D. R. Lynch and K. D. Paulsen, "Origin of Vector Parasites in Numerical Maxwell Solutions," **IEEE Trans. on Microwave Theory and Techniques**, Vol. 39, No. 3, March 1991, pp. 383-394.

[3] D. R. Lynch and K. D. Paulsen, "Elimination of Vector Parasites in Finite Element Maxwell Solutions," **IEEE Trans. on Microwave Theory and Techniques**, Vol. 39, No. 3, March 1991, pp. 395-404.

[4] P. P. Silvester and R. L. Ferrari, **Finite Elements for Electrical Engineers, 2nd ed.**, Cambridge University Press, Cambridge, England, 1989.

[5] O. C. Zienkiewicz and R. L. Taylor, **The Finite Element Method, 4th ed.**, McGraw Hill, New York, 1989.

[6] K. D. Paulsen, D. R. Lynch, and J. W. Strohbehn, "Three-Dimensional Finite, Boundary, and Hybrid Element Solutions of the Maxwell Equations for Lossy Dielectric Media," **IEEE Trans. on Microwave Theory and Techniques**, Vol. 36, No. 4, April 1988, pp. 682-693.

[7] DesignCAD 3-D is a product of American Small Business Computers, Inc.; 327 South Mill St.; Pryor, OK. 74361. Phone: 918-825-4844.

[8] T. H. Hubing and G. K. Bhat, "Using Commercial CAD Packages to Interface with 3-D EM Modeling Codes," **Proc. of the 8th Annual Review of Progress in Applied Computational Electromagnetics**, Monterey, CA, March 1992, pp. 607-610.